Journal of Polymers and the Environment (2022) 30:4193–4200
https://doi.org/10.1007/s10924-022-02491-5

ORIGINAL PAPER

Poly (Vinyl Alcohol) Composite Membrane with Polyamidoamine Dendrimers for Efficient Separation of CO_2/H_2 and CO_2/N_2

Yaxin Zhao[1] · Huafeng Tian[1] · Yuge Ouyang[1] · Aimin Xiang[1] · Xiaogang Luo[2] · Xingwei Shi[3] · Songbai Ma[4]

Accepted: 18 May 2022 / Published online: 27 June 2022

Abstract

Although polyvinyl alcohol (PVA) membranes are commonly used for CO_2 separation, there is still large development space in mechanical properties and high selectivity of the gas separation process. In this study, the gas separation performance and mechanical properties of the (PVA/Cu^{2+}) substrate membranes were improved by introducing polyamidoamine (PAMAM). PAMAM had an important effect on the gas adsorption and separation performance of the membrane. In addition, the gas adsorption and separation properties of the PVA/Cu^{2+}/PAMAM membrane (PPCm) were analyzed and studied when the inlet gas pressure and the species of mixed gases were variable. The results showed that the crystallinity and mechanical properties of the membrane with the PAMAM had been significantly improved. Young's modulus of PPCm with 30% PAMAM was 132% higher than that of the PVA/Cu^{2+} composite membrane without PAMAM. In addition, efficient separation efficiency and high selectivity of the gas separation process were observed. The separation factors of the PPCm for CO_2/H_2 and CO_2/N_2 were about three times higher than that of the PVA/Cu^{2+} substrate membranes. These results suggested that the introduction of PAMAM was promising for CO_2 separation and permeance.

Keywords PVA · PAMAM · Carrier · Crystallinity · CO_2 separation

Introduction

With the increasingly severe climate change, the separation of carbon dioxide from its emission sources has attracted global attention. Efforts have been made to find economic separation techniques to capture and separate CO_2 [1–5]. Many CO_2 capture technologies have been developed, among which membrane separation is one of the most effective technologies. Compared with the traditional method of solvent absorption, membrane separation technology has the advantages of low investment cost, compact structure and no secondary pollution [6–8]. Polyvinyl alcohol (PVA) membrane is generally used in the mixed gas separation, because it has the large amount of the hydroxyl groups on its surface, which is conducive to the formation of a large diffusion rate difference in the membrane [9–13]. Nevertheless, the separation efficiency and mechanical properties of the membrane are still poor, and it cannot be commercially applied. The in-depth study of PVA membranes found that some metal ions with PVA could form macromolecular complexes [14–19]. Therefore, the mechanical properties of the PVA based membrane were further improved by introducing Cu^{2+} into the PVA membrane [10]. But its gas separation efficiency still needs to be improved.

✉ Huafeng Tian
tianhuafeng@th.btbu.edu.cn

✉ Xiaogang Luo
xgluo@wit.edu.cn

✉ Xingwei Shi
xwshi@ipe.ac.cn

[1] Beijing Key Laboratory of Quality Evaluation Technology for Hygiene and Safety of Plastics, School of Chemical and Material Engineering, Beijing Technology and Business University, Beijing 100048, China

[2] Hubei Key Laboratory of Novel Reactor and Green Chemistry Technology, School of Chemical Engineering and Pharmacy, Wuhan Institute of Technology, Wuhan, China

[3] Beijing Key Laboratory of Ionic Liquids Clean Process, CAS Key Laboratory of Green Process and Engineering, Institute of Process Engineering, Chinese Academy of Sciences, Beijing 100190, China

[4] School of E-Business and Logistics, Beijing Technology and Business University, Beijing 100048, China

Besides, there is a constraint trade-off between permeability and selectivity of commonly used polymer membranes. Polymer membranes with high permeability are usually less selective [20–23]. The promotion transfer membrane is to introduce the carrier inside the membrane, which is connected to the base membrane in the form of covalent bond. And then to promote the transfer of the component by reversible interaction between the carrier and a specific gas component in the mixed gases to be separated. Moreover, it may be mentioned that the carrier in the membrane is connected to the substrate in the form of covalent bond, which effectively solves the immobilization problem of the carrier [24, 25].

Polyamidoamine (PAMAM) is one of the most widely studied and mature tree-like molecules. It has high branching degree, symmetrical radial structure, high group density of surface amine groups. PAMAM can provide a large number of primary and secondary amine reaction active points, and has good hydrodynamic properties, easy membrane formation, good compatibility with PVA and so on [26–28].

In this work, based on the high permeability and selectivity of CO_2, PAMAM was introduced into PVA/Cu^{2+} membranes to prepare the PVA/PAMAM/Cu^{2+} promoting transfer membrane (PPCm) for further exploration. PAMAM could provide a large number of reversible reaction points with carbon dioxide. It was found that without affecting the permeability, the selection of CO_2 was highly improved. It provided a solution for the membrane to weaken the constraint trade-off between permeability and selectivity of it.

Experiment

Materials

PVA (117) was purchased from Kuraray Co.Ltd. $CuSO_4{\cdot}5H_2O$ (Analytical Reagent) was from Beijing Sinopharm Chemical Reagent Co., Ltd. Polyethersulfone (PES005) was from Beijing Vontron Technology Co., Ltd. PAMAM (zero-generation) was self-made in laboratory.

Preparation of the PPCm

PVA aqueous solution with solid content of 5% was prepared. Then different contents of PAMAM were added into PVA solution by stirring 4 h at room temperature. The calculation formula of PAMAM content (w_{PAMAM}) is as follows:

$$w_{PAMAM} = \frac{m_{PAMAM} \times 100\%}{m_{pamam} + m_{PVA} + m_{Cu^{2+}}}$$

The m_{PAMAM}, m_{PVA}, $m_{Cu}{}^{2+}$ are the mass of PAMAM, PVA, Cu^{2+}.

Whereafter, 5% Cu^{2+} was added into PVA/PAMAM solution by stirring 2 h at room temperature. Then the solution was allowed to stand for a period of time to remove the bubbles. The PVA/PAMAM/Cu^{2+} membrane-forming solution was poured horizontally into the glass mold to get the PVA/PAMAM/Cu^{2+} promoting transfer membrane (PPCm). Finally, the PPCm was dried at 60 ℃ for 24 h.

Characterization

The structure of the PPCm was determined by Fourier transform infrared spectrometer (FTIR). The infrared scanning test was carried out by potassium bromide pressing method and Nicolet iN10MX (Thermo Electron, US) infrared tester. The scanning range was 4000–500 cm^{-1}.

The structure of dried PPCm was observed and photographed with scanning electron microscope (SEM) (Quanta FEG-250, FEI Nanoports, US) operating at an acceleration voltage of 10 kV.

The dried samples were tested with Different Scanning Calorimety (DSC) (Q2500 TA Instruments) in the N_2 atmosphere. And the sample weight was about 5–10 mg.

The mechanical properties test, the splines were placed 24 h before testing. And it tested by the tensile speed of 50 mm/min at room temperature. During the experiment, each group of samples was tested 5 times, and the average value was taken.

Gas permeability and separation performance test: effective sample size: Φ97 mm, transmission area: 38.48 cm^2 and gas test pressure: 0.5 MPa for the single gases CO_2, N_2 and H_2. Effective transmission area: 19.26 cm^2 and gas test pressure: 0.1 MPa–0.5 MPa for mixed gases CO_2/N_2 with a volume radio of 85/15 and CO_2/H_2 with a volume radio of 50/50. The adsorption separation chamber was sealed with a sealing ring to ensure that the gas on the permeace side did not diffuse with the air during the test.

2. Results and Discussion

Figure 1 illustrated the schematic for the preparation of the PVA/Cu^{2+}/PAMAM membranes (PPCm) and the process of gases separation. PAMAM has high concentrations of amine groups which can enable the membrane to increase the selectivity of CO_2. Therefore, PAMAM was introduced into the PVA/Cu^{2+} membranes. Cu^{2+} and PAMAM complexed with PVA polymer chains to form the PPCm with significantly enhanced mechanical properties and separation efficiency [7, 8]. Generally, small molecular gases such as CO_2, N_2 and H_2 permeated through the membrane by the physical solution-diffusion mechanism. However, when PAMAM was introduced into the membrane, the amine groups in PAMAM

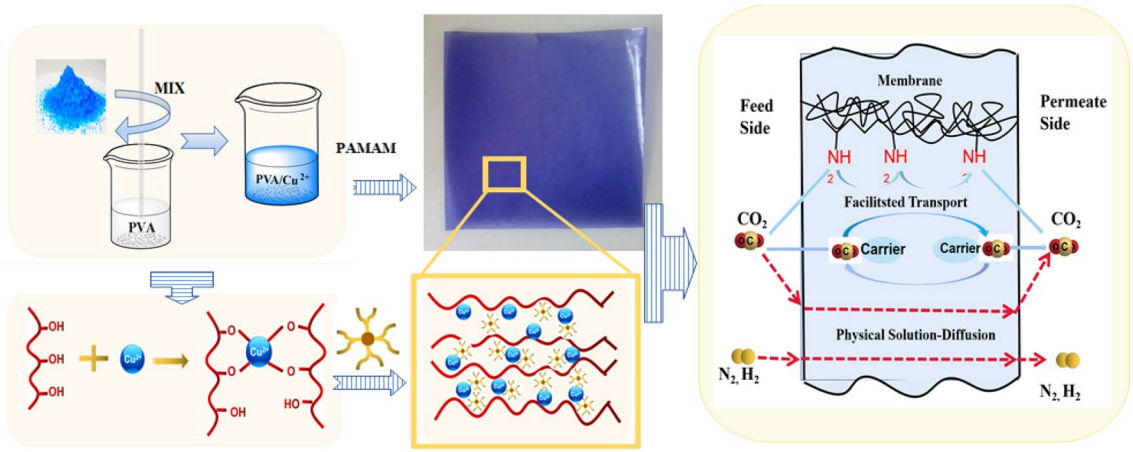

Fig. 1 The schematic for preparation of the PPCm and the process of gases separation

could react reversibly with CO_2, so as to promote the permeance and separation of CO_2.

Structure Characterization

Figure 2 showed the FTIR spectra of PPCm with different PAMAM contents. For the PVA/Cu^{2+} base membranes without PAMAM, there was 3416 cm^{-1} stretching vibration attributed to -OH, 2919 cm^{-1} stretching vibration attributed to -C-H, the stretching vibration of 1434 cm^{-1} was H–C–H, 912 cm^{-1} and 842 cm^{-1} belonged to the stretching vibration of C–O–H and C–C respectively. But for the PPCm two new absorption peaks position at 1645 cm^{-1} and 1565 cm^{-1} belonged to the stretching vibration of –C–O– and bending vibration of –N–H in PAMAM. With the increase of PAMAM, they shifted to 1655 cm^{-1} and 1555 cm^{-1}. At this time, the peak position of –OH gradually moved to a lower wave number. The shift of these functional group peaks was mainly due to the hydrogen bond interaction between the –NH–CO- group in the PAMAM and the –OH group in the PVA. The strong hydrogen bonding interaction could act as physical crosslinking agents, which would enhance the mechanical performances of the matrix.

Figure 2(b) showed the surface and cross-section SEM images of PPCM with different PAMAM contents. When the content of PAMAM was 0% and 5%, the cross-section and surface of the membrane were smooth, and no obvious PAMAM agglomeration was observed. However, when the content of PAMAM exceeds 10%, it was obvious that the agglomeration phenomenon was more and more obvious on the surface, and the aggregate was also larger and larger. The cross section of the membrane was also rougher. The results showed that with the increase of PAMAM content, the surface roughness of PPCM increases, resulting in the decrease of membrane homogenization. This also led to a decrease in the tensile strength of the membrane.

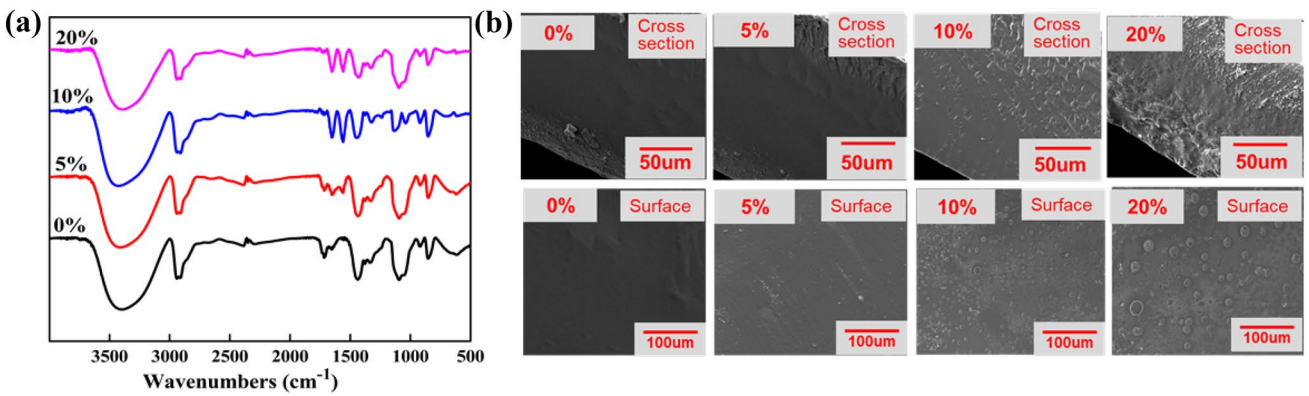

Fig. 2 **a** the FTIR spectra and **b** the surface and cross-section SEM images of PPCm with different PAMAM contents

DSC Analysis

Figure 3 showed the DSC curves and crystallinity of PPCm with different PAMAM contents. From the endothermic curves of the PPCm, PVA crystallization peak at ca. 180 ℃ could be observed. With the introduction of PAMAM, the crystallization onset temperature and the crystallization peak temperature decreased with the increase of PAMAM. The crystallinity of PPCm could be calculated from the follows:

$$X_c = \frac{\Delta H_c}{f \times \Delta H_0} \times 100\%$$

ΔH_0 is the melting enthalpy of the PVA membrane at 100% crystallinity; the ΔH_c is the melting enthalpy of the transfer membrane; and the *f* is the mass fraction of the polymer matrix.

It could be concluded that the crystallinity of PPCm was obviously higher than that of PVA/Cu^{2+} based membrane without PAMAM, as shown in Fig. 3(c). With the increase of PAMAM, the crystallinity of PPCm increased obviously. The results showed that the PAMAM with high degree of branching exhibited heterogeneous nucleation effect in the PVA matrix, which could increase the crystallinity.

Mechanical Properties

Figure 4 illustrated tensile strength, Young's modulus and elongation at break of the PPCm with different PAMAM contents. Figure 4 showed that the tensile strength of 5% PAMAM increased to the maximum. And then the tensile strength of PPCm decreased continuously with the increase of PAMAM content. PAMAM exhibited reinforcing effect in the matrix, and increased the rigidity of the membrane. With the increase of PAMAM, the Young's modulus of PPCm increased obviously. When the content of PAMAM in the membrane was 30%, the Young's modulus reached 648.6 MPa. The Young's modulus of the film without PAMAM was only 279.5 MPa. The Young's modulus of the transfer promoting membrane with the 30% PAMAM content increased by 132% compared with the PVA/Cu2 + base membrane without PAMAM. The main reason was that the crystallinity of the membranes increased with the increasing of PAMAM. As the crystallinity of the membrane increased, its Young's modulus will increase accordingly. The fracture elongation of PPCm decreased significantly with the increase of PAMAM content. When the existence of PAMAM was too much, it destroyed the structure of the membrane, resulting in the decrease of tensile strength and elongation at break. Besides, the results of Young's modulus and tensile strength were mainly due to the increase of crystallinity of the PPCm, as well as the strong hydrogen bonding interactions. The raise of intermolecular force leaded to the promotion of Young's modulus and the decline of tensile strength.

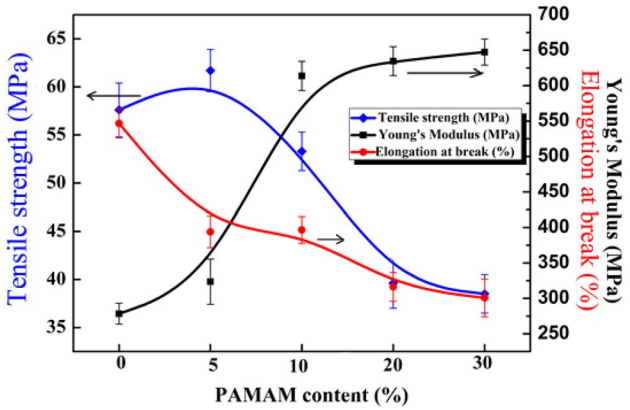

Fig. 4 Tensile strength, Young's Modulus and Elongation at break of the PPCm with different PAMAM contents

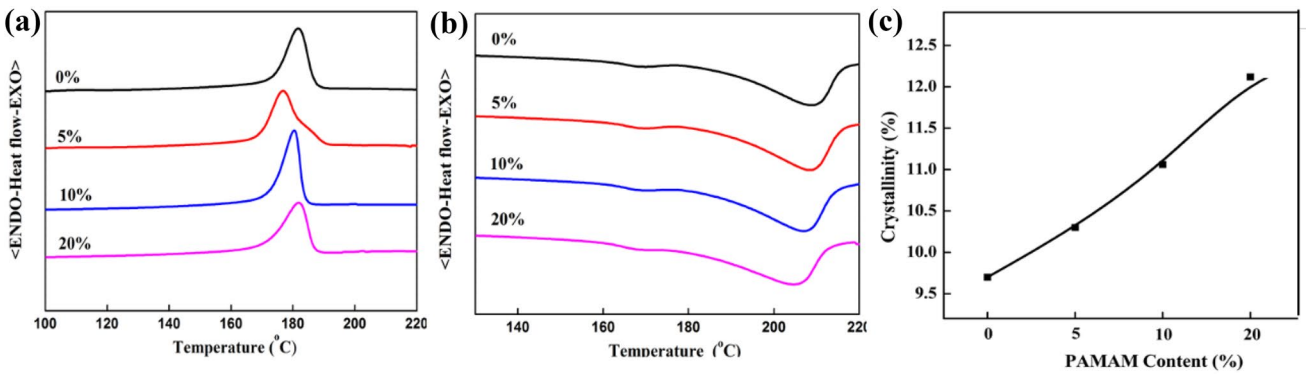

Fig. 3 DSC **a** heating curves **b** cooling curves and **c** Crystallinity of PPCm with different PAMAM contents

Gas Permeance Properties

Separation Properties for a Single Gas

The gas permeance unit (GPU) of three single gases, CO_2, H_2 and N_2, were measured, as shown in the Fig. 5. The CO_2 GPU of the PPCm increased with the increase of PAMAM. The gas permeance unit of CO_2 was as high as 120 GPU when the PAMAM concentration was 30%. It was much greater than that of N_2 and H_2. Even with the increase of PAMAM concentration, the gas permeance unit slightly decreased. The small decrease of gas permeance of N_2 and H_2 was related to the increase of PAMAM content. It was mainly due to the reduction of physical solution-diffusion in the process of gas permeance. The crystallinity of the membrane increased and the molecular chain arrangement orientation made the membrane more compact, so the small molecules that could be physically penetrated were reduced. Therefore, the physical solution-diffusion of the membrane decreased with the PAMAM content increasing. However, in the course of CO_2 permeance through PPCm with amine carriers, there was not only physical solution-diffusion mechanism, but also facilitated transport mechanism. This fully illustrated that the introduction of PAMAM would have an efficient effect on the separation of mixed gases.

Separation Properties of the Mixed Gas

As shown in Fig. 6, the gas permeance unit of CO_2/N_2 with a volume ratio of 15/85 was measured under different inlet gas pressures. The GPU of CO_2 and N_2 increased significantly with the increase of PAMAM contents. And the CO_2 and N_2 permeance unit increased at higher inlet gas pressure. When the PAMAM was 10% and the inlet gas pressure was 0.5 MPa, the CO_2 permeance unit was 7.3 GPU and the N_2 permeance unit was 1.6 GPU, as illustrated in Fig. 6 (a, b). Separation factor was an important parameter to measure the separation ability of membranes. The separation factors for the CO_2/N_2 gas mixture of PPCm were calculated, as shown in Fig. 6(c). The separation factors of PPCm could be calculated from the follows:

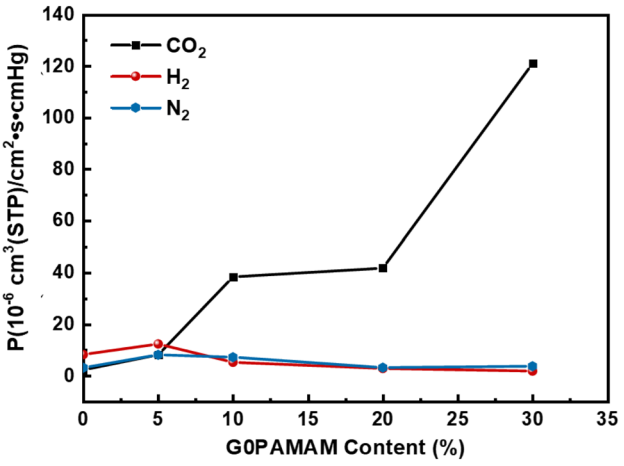

Fig. 5 The gas permeance unit of the PPCms with different PAMAM contents

$$\alpha = \frac{y_A/y_B}{X_A/X_B}$$

y_A is the volume fraction of component A in the detection gas (including permeability and purge gas); y_B is the volume fraction of component B in the detection gas (including permeability and purge gas); X_A is the volume fraction of component A in the feed gas; X_B is the volume fraction of component B in the feed gas.

As the PAMAM content increasing, the separation factor of CO_2/N_2 increased obviously. When the content of amine was too much, its steric resistance increases, resulting in the decrease of air filtration efficiency.

The permeance of small molecular gases such as CO_2 and N_2 through the membrane was the physical-diffusion mechanism. Beyond that, there was another facilitated transport mechanism for CO_2 permeance through the PPCm. Therefore, the gas permeance unit of CO_2 was obviously larger than that of the N_2. And with the increase of PAMAM contents, the separation factor increased. Because it increased the density of effective amine groups which were capable of interacting with CO_2. The CO_2 and N_2 permeance unit increased at higher inlet gas pressure, because of the coupling of two gases in the mixture. In general, the separation factors of PPCm increased with the increase of PAMAM.

The general trade-off between polymer permeability and selectivity was first quantified by Robeson when he identified 16 s in plots of log (P_x/P_y) versus log (P_x). Robeson updated all of the upper bounds in 2008 using initial data for two spirobisindane-based Polymers of Intrinsic Microporosity. Among them, the upper limit of CO_2/N_2 was updated again by McKeown et al. in 2019. Fitting parameters for the 2008 and proposed CO_2/N_2 and CO_2/H_2 upper bounds using the formula:

$$p_x = k\alpha_{xy}^n$$

where P_x is permeability of the most permeable x-gas, k is the front factor, α_{xy} is the selectivity for x/y gas pair, and n is the slope.

In Fig. 6(d), under the same 1 bar = 0.1 MPa, the comparison of the CO_2 separation performance in this work with the upper bounds in the literature [11, 20] was showed. The PCO_2/PN_2 in the work was numerically close to the upper bounds in the literatures. Therefore, as the gas separation membrane was qualified.

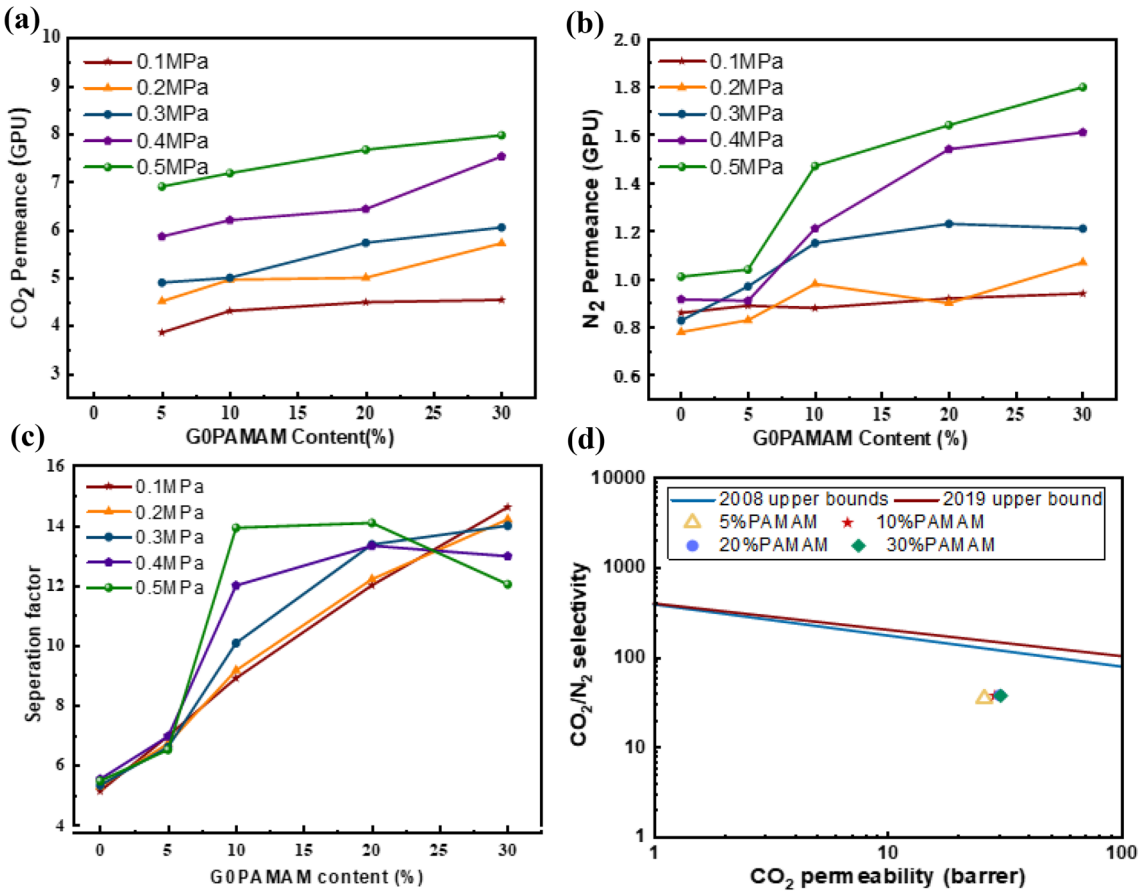

Fig. 6 CO_2/N_2 mixture separation performance of the membranes with different PAMAM concentrations. **a** CO_2 permeance, **b** N_2 permeance, and **c** the separation factors of the CO_2 /N_2; **d** comparison of the membranes with 5%, 10%, 15% and 20% PAMAM performance in this work with literature data [11, 20] for CO_2/N_2. Feed gas: CO_2/N_2 (15/85 by volume) mixture

Under different inlet gas pressures, the gas permeance unit of CO_2/H_2 with a volume ratio of 50/50 was illustrated in Fig. 7(a, b). The CO_2 permeance unit generally decreased and then stabilized with the increase of PAMAM content, while the H_2 permeance unit generally decreased with the increase of PAMAM content. The CO_2/H_2 separation factors of the PVA/PAMAM/Cu^{2+} transfer membranes were calculated, as shown in Fig. 7(c). And when the PAMAM was 20% and the inlet gas pressure was 0.5 MPa, the separation factor of the PPCm was 1.3, reaching the maximum. It was in the upper part of diffusivity coefficient CO_2/N_2 lie between 0.9 and 1.5 proposed by McKeown et al. The separation factor of CO_2/H_2 increased steadily, with the increase of PAMAM contents. When the PAMAM content exceeded 20%, the separation factor of PPCm for CO_2/H_2 decreased.

Since the dynamic diameter of the H_2 molecule is smaller than that of the CO_2 molecule [29]. The small size of H_2 molecule was easier to permeate through the membrane than CO_2 and N_2 molecules by the dissolution-diffusion mechanism, when the PAMAM content increased, the tightness of the membrane increased, resulting in the decline of H_2 permeance unit. However, CO_2 mainly permeated through the PPCm by the facilitated transport mechanism. Therefore, the separation factor of the PPCm for the CO_2/H_2 mixture was much smaller than that for CO_2/N_2. When the PAMAM content was too much, the effective amine density decreased. And it had resulted in the decline of the separation factors.

In Fig. 7(d), under the same 1 bar = 0.1 MPa, the comparison of the CO_2 separation performance in this work was compared with the upper bound in the literature [20]. And the numerical gap between the CO_2/H_2 separation performance of the membranes in this work and the upper bound was bigger than that between the CO_2/N_2 separation performance of the membranes in this work and the upper bound in the literature.

Conclusion

In this study, PAMAM was successfully introduced into the PVA/Cu^{2+} base membrane, and the uniformly transparent PPCm was successfully prepared. PAMAM could act

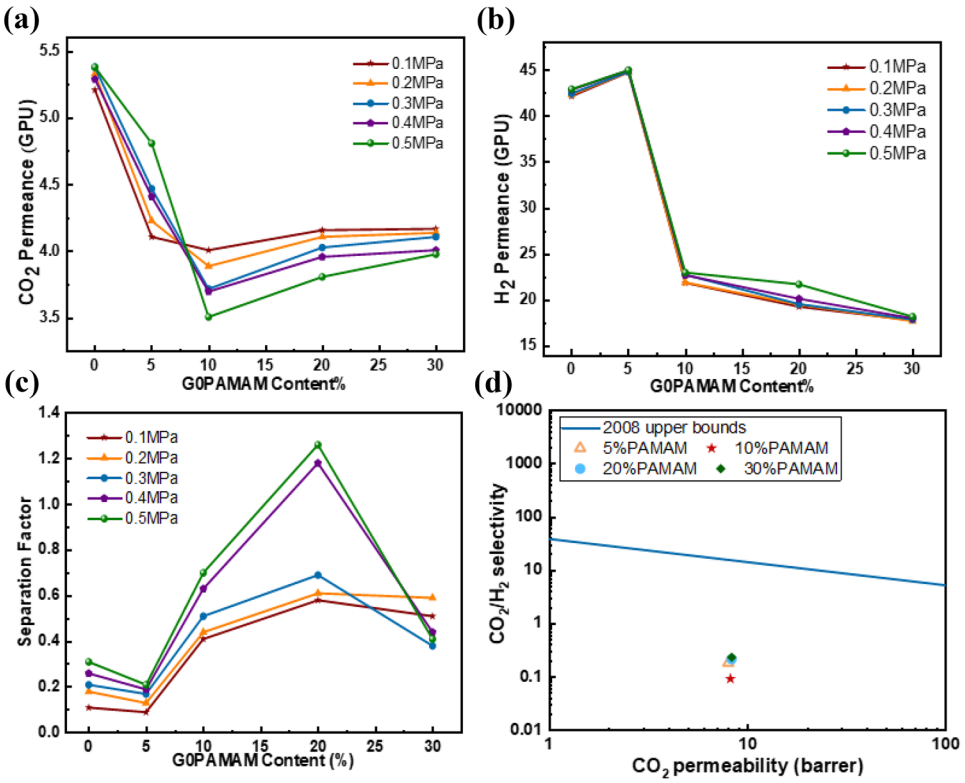

Fig. 7 CO_2/H_2 mixture separation performance of the membranes with different PAMAM concentrations. **a** CO_2 permeance, **b** H_2 permeance, and **c** the separation factors of the CO_2 / H_2; **d** comparison of the membranes with 5%, 10%, 15% and 20% PAMAM performance in this work with literature data [20] for CO_2/H_2. Feed gas: CO_2/H_2 (50/50 by volume) mixture

as heterogeneous nucleation agents in the PVA/Cu^{2+} base membrane to improve the crystalstallization of the transfer membrane. The introduction of the mechanical properties of PAMAM reduced the fracture elongation and increased the elastic modulus. The introduction of PAMAM has little effect on the gas permeance unit (GPU) of N_2 and H_2. But it significantly improved the GPU of CO_2. As the content of PAMAM increased, the separation factor of PPCm of CO_2/N_2 and CO_2/H_2 were increased. The separation factor of PPCm of CO_2/N_2 was much larger than that of CO_2/H_2. This membrane can be used for CO_2 capture and separation, and it will make an important contribution to the greenhouse effect.

Acknowledgements This work was supported by Beijing Natural Science Foundation (2202014), School Level Cultivation Fund of Beijing Technology and Business University for Distinguished and Excellent Young Scholars (BTBUYP2021), funding of Hubei key Laboratory of Novel Reactor and Green Chemical Technology (Wuhan Institute of Technology).

Funding The authors have not disclosed any funding.

Declarations

Competing Interest The authors declare that they have no known competing financial interests or personal relationships that could have appeared to influence the work reported in this paper.

References

1. Torstensen JØ, Helberg RML, Deng L, Gregersen ØW, Syverud K (2019) PVA/nanocellulose nanocomposite membranes for CO_2 separation from flue gas. Int J Greenh Gas Control 81:93–102. https://doi.org/10.1016/j.ijggc.2018.10.007
2. Maheswari AU, Palanivelu K (2017) Separation of carbon dioxide and nitrogen gases using novel composite membranes. Can J Chem 95(1):57–67. https://doi.org/10.1139/cjc-2016-0090
3. Iyer GM, Liu L, Zhang C (2020) Hydrocarbon separations by glassy polymer membranes. J Polym Sci 58(18):2482–2517. https://doi.org/10.1002/pol.20200128
4. Francisco GJ, Chakma A, Feng X (2007) Membranes comprising of alkanolamines incorporated into poly(vinyl alcohol) matrix for CO_2/N_2 separation. J Membr Sci 303(1–2):54–63. https://doi.org/10.1016/j.memsci.2007.06.065
5. Wang Z, Pan Z (2015) Preparation of hierarchical structured nanosized/porous poly(lactic acid) composite fibrous membranes for air filtration. Appl Surf Sci 356:1168–1179. https://doi.org/10.1016/j.apsusc.2015.08.211
6. Liu H, Liang X (2011) Strategy for promoting low-carbon technology transfer to developing countries: the case of CCS. Energy

Policy 39(6):3106–3116. https://doi.org/10.1016/j.enpol.2011.02.051
7. Taniguchi I, Kinugasa K, Toyoda M, Minezaki K (2017) Effect of 8 structure on CO_2 capture by polymeric membranes. Sci Technol Adv Mater 18(1):950–958. https://doi.org/10.1080/14686996.2017.1399045
8. Mondal A, Barooah M, Mandal B (2015) Effect of single and blended amine carriers on CO_2 separation from CO_2 /N_2 mixtures using crosslinked thin-film poly(vinyl alcohol) composite membrane. Int J Greenh Gas Control 39:27–38. https://doi.org/10.1016/j.ijggc.2015.05.002
9. Shirvani H, Sadeghi M, Taheri Afarani H, Bagheri R (2018) Polyurethane/poly(vinyl alcohol) blend membranes for gas separation. Fibers Polym 19(5):1119–1127. https://doi.org/10.1007/s12221-018-1023-6
10. Liu Q, Ge X, Xiang A, Tian H (2016) Effect of copper sulfate pentahydrate on the structure and properties of poly(vinyl alcohol)/graphene oxide composite films. J Appl Polym Sci. https://doi.org/10.1002/app.44135
11. Comesaña-Gándara B, Chen J, Bezzu CG, Carta M, Rose I, Ferrari MC, Esposito E, Fuoco A, Jansen JC, McKeown NB (2019) Redefining the Robeson upper bounds for CO_2/CH_4 and CO_2/N_2 separations using a series of ultrapermeable benzotriptycene-based polymers of intrinsic microporosity. Energy Environ Sci 12(9):2733–2740
12. Lilleby Helberg RM, Dai Z, Ansaloni L, Deng L (2020) PVA/PVP blend polymer matrix for hosting carriers in facilitated transport membranes: synergistic enhancement of CO_2 separation performance. Green Energy Environ 5(1):59–68. https://doi.org/10.1016/j.gee.2019.10.001
13. Jahan Z, Niazi MBK, Hägg M-B, Gregersen ØW (2018) Cellulose nanocrystal/PVA nanocomposite membranes for CO_2/CH_4 separation at high pressure. J Membr Sci 554:275–281. https://doi.org/10.1016/j.memsci.2018.02.061
14. Edubilli S, Gumma S (2019) A systematic evaluation of UiO-66 metal organic framework for CO_2/N_2 separation. Sep Purif Technol 224:85–94. https://doi.org/10.1016/j.seppur.2019.04.081
15. Shakeel I, Hussain A, Farrukh S (2019) Effect analysis of nickel ferrite ($NiFe_2O_4$) and titanium dioxide (TiO_2) nanoparticles on CH_4/CO_2 gas permeation properties of cellulose acetate based mixed matrix membranes. J Polym Environ 27(7):1449–1464. https://doi.org/10.1007/s10924-019-01442-x
16. Deeksha B, Sadanand V, Hariram N, Rajulu AV (2021) Preparation and properties of cellulose nanocomposite fabrics with in situ generated silver nanoparticles by bioreduction method. J Bioresources Bioproducts 6(1):75–81. https://doi.org/10.1016/j.jobab.2021.01.003
17. Barooah M, Mandal B (2019) Synthesis, characterization and CO_2 separation performance of novel PVA/PG/ZIF-8 mixed matrix membrane. J Membr Sci 572:198–209. https://doi.org/10.1016/j.memsci.2018.11.001
18. Niazi MBK, Jahan Z, Ahmed A, Rafiq S, Jamil F, Gregersen ØW (2020) Effect of Zn-Cyclen mimic enzyme on mechanical, thermal and swelling properties of cellulose nanocrystals/PVA nanocomposite membranes. J Polym Environ 28(7):1921–1933. https://doi.org/10.1007/s10924-020-01737-4
19. Ashok B, Hariram N, Siengchin S, Rajulu AV (2020) Modification of tamarind fruit shell powder with in situ generated copper nanoparticles by single step hydrothermal method. J Bioresources Bioproducts 5(3):180–185. https://doi.org/10.1016/j.jobab.2020.07.003
20. Robeson LM (2008) The upper bound revisited. J Membr Sci 320(2008):390–400
21. Fadhel B, Hearn M, Chaffee A (2009) CO_2 adsorption by PAMAM dendrimers: significant effect of impregnation into SBA-15. Microporous Mesoporous Mater 123(1–3):140–149. https://doi.org/10.1016/j.micromeso.2009.03.040
22. Dutcher B, Fan M, Russell AG (2015) Amine-based CO_2 capture technology development from the beginning of 2013-a review. ACS Appl Mater Interfaces 7(4):2137–2148. https://doi.org/10.1021/am507465f
23. Barooah M, Mandal B (2018) Enhanced CO_2 separation performance by PVA/PEG/silica mixed matrix membrane. J Appl Polym Sci. https://doi.org/10.1002/app.46481
24. Gong P, Zhao Y, Li K, Tian H, Li C (2021) Effect of plasticizer content on the structure and properties of SPI/MA-g-PBAT blend films. J Polym Environ. https://doi.org/10.1007/s10924-021-02223-1
25. Li K, Fan G, Tian H, Yuan L, Yao Y, Xiang A, Luo X (2021) Highly oriented thermoplastic Poly (vinyl alcohol) films by uniaxial drawing: effect of stretching temperature and draw ratio. J Polym Environ 29(10):3263–3270. https://doi.org/10.1007/s10924-021-02113-6
26. Wang X, Chen H, Zhang L, Yu R, Qu R, Yang L (2014) Effects of coexistent gaseous components and fine particles in the flue gas on CO_2 separation by flat-sheet polysulfone membranes. J Membr Sci 470:237–245. https://doi.org/10.1016/j.memsci.2014.07.040
27. Niazi MBK, Jahan Z, Berg SS, Gregersen OW (2017) Mechanical, thermal and swelling properties of phosphorylated nanocellulose fibrils/PVA nanocomposite membranes. Carbohydr Polym 177:258–268. https://doi.org/10.1016/j.carbpol.2017.08.125
28. Klepić M, Setničková K, Lanč M, Žák M, Izák P, Dendisová M, Fuoco A, Jansen JC, Friess K (2020) Permeation and sorption properties of CO_2-selective blend membranes based on polyvinyl alcohol (PVA) and 1-ethyl-3-methylimidazolium dicyanamide ([EMIM][DCA]) ionic liquid for effective CO_2/H_2 separation. J Membr Sci. https://doi.org/10.1016/j.memsci.2019.117623
29. Dong S, Wang Z, Sheng M et al (2020) High-performance multilayer composite membrane with enhanced interlayer compatibility and surface crosslinking for CO2 separation[J]. J Membr Sci 610:118221